Supplementary Information for:

Sugar-alcohol@ZIF nanocomposites display suppressed phase-change temperatures

Lukas Hackl[1,2,$], Chih-Hao Hsu[1,$], Madeleine P. Gordon[1,3], Kelly Chou[1,4], Canghai Ma[1], Matthew Kolaczkowski[1,4], Christopher L. Anderson[1,4], Yi-Sheng Liu[5], Jinghua Guo[5], Peter Ercius[1], Jeffrey J. Urban[1,*]

[1] The Molecular Foundry, Lawrence Berkeley National Lab, 1 Cyclotron Road, Berkeley, CA 94720, USA

[2]Department of Civil and Environmental Engineering, 760 Davis Hall, Berkeley, CA 94720, USA

[3]Applied Science and Technology Graduate Group, University of California Berkeley, 210 Hearst Memorial Mining Building, Berkeley, CA 94720, USA

[4]Department of Chemistry, 419 Latimer Hall, University of California Berkeley, CA 94720, USA

[5]Advanced Light Source, Lawrence Berkeley National Lab, 1 Cyclotron Road, Berkeley, CA 94720, USA

[$]Denoting equal contribution

**corresponding author, email: jjurban@lbl.gov*

Supplementary Tables

Table S1. Molar concentrations of Methyl- and Vinylimidazole molecules contained in different acid-digested SA@ZIF samples, normalized to molar erythritol concentrations, determined via NMR analysis outlined in Figure S9-11 below.

ZIF	Methylimidazole (MIm)	Vinylimidazole (VIm)	Erythritol (E)	MIm/VIm	E/MIm	E/VIm
EZV	10.1	0.47	1	0.05	0.10	2.13
EZV-PEG	9.52	1.91	1	0.2	0.11	0.52
EZV-PFT	5.25	0.27	1	0.05	0.19	3.77

SUPPLEMENTARY FIGURES

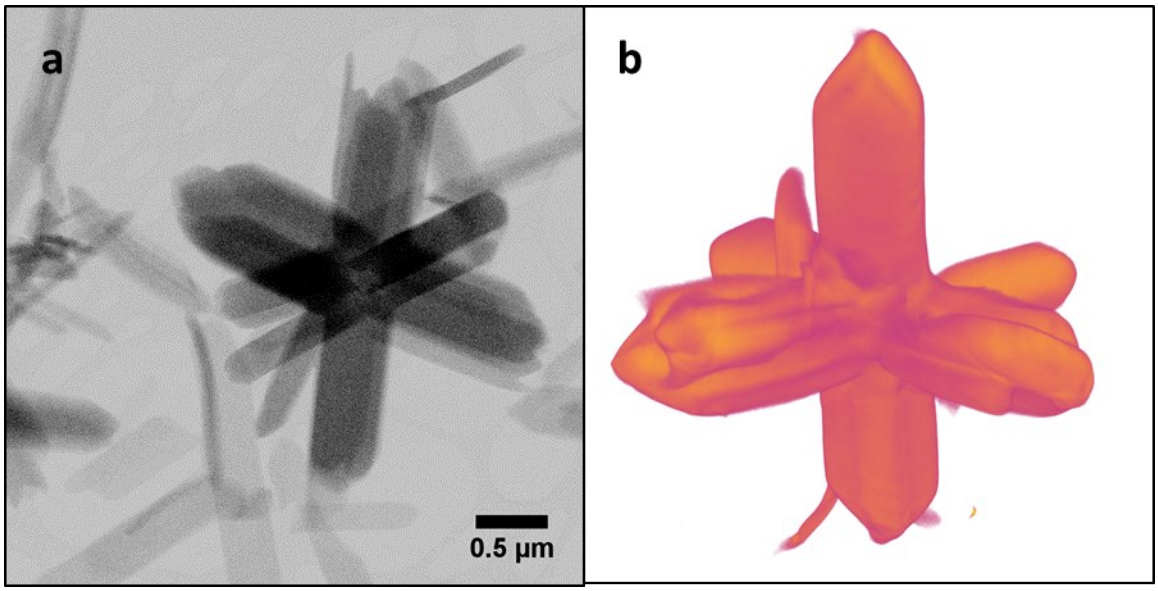

Figure S1. a. STEM image of EZ synthesized at 200 °C for 4 hours and the corresponding b. tomography 3D model. The tomography was reconstructed based on static STEM images with various tilted angle (+70° to -70° with a 2° step) and using Ag nanoparticles as markers to align STEM images.

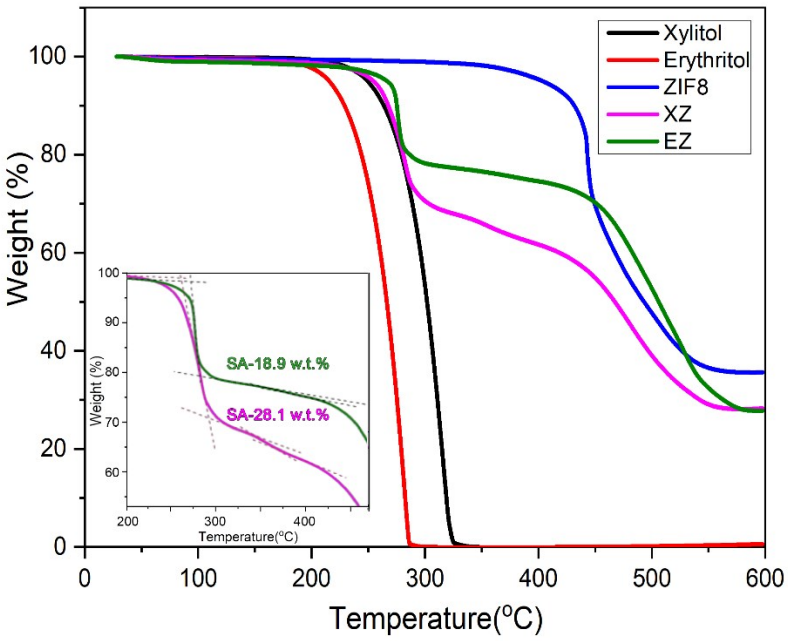

Figure S2. Sample weight loss as per TGA data of EZ, XZ, ZIF-8 and bulk erythritol and xylitol samples.

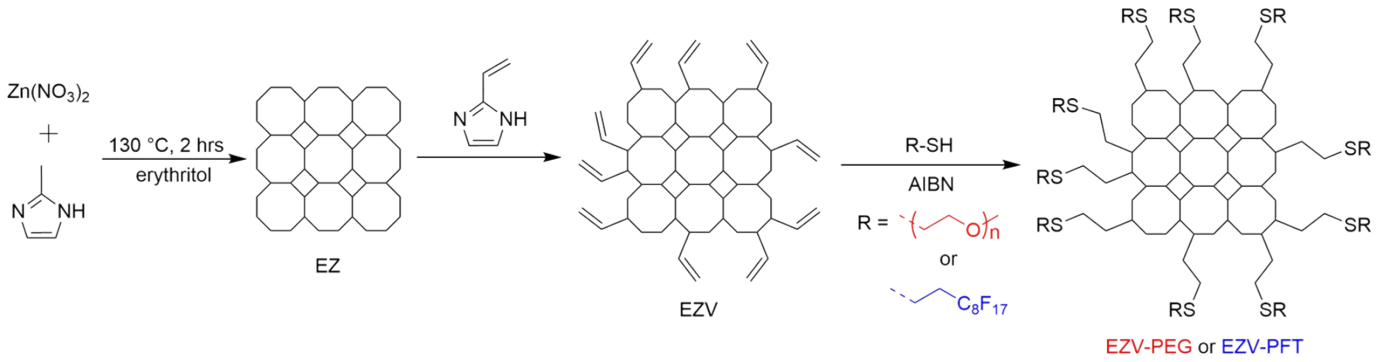

Figure S3. Synthesis cartoon for surface functionalization of EZV crystals with PEG and PFT molecules.

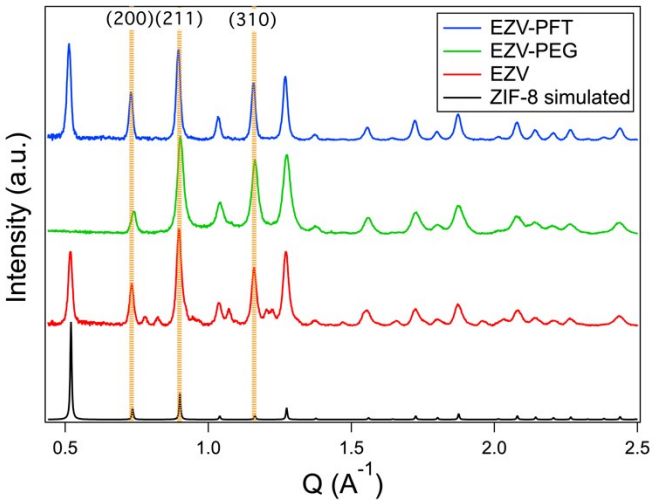

Figure S4. XRD diffraction patterns for pellet pressed surface-functionalized (EZV-PFT, EZV-PEG) and unfunctionalized (EZV) crystals in comparison to simulated ZIF-8 pattern.

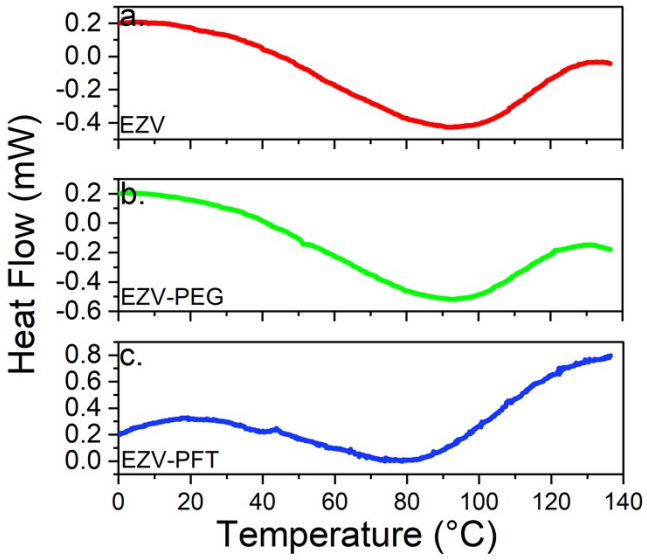

Figure S5. Thermal analysis of encapsulated samples by DSC. Heat flow into a. EZV, b. EZV-PEG, and c. EZV-PFD. The thermal point of phase transition for all three crystal assemblies, both with and without polymer encapsulation, remains depressed compared to that of pure erythritol.

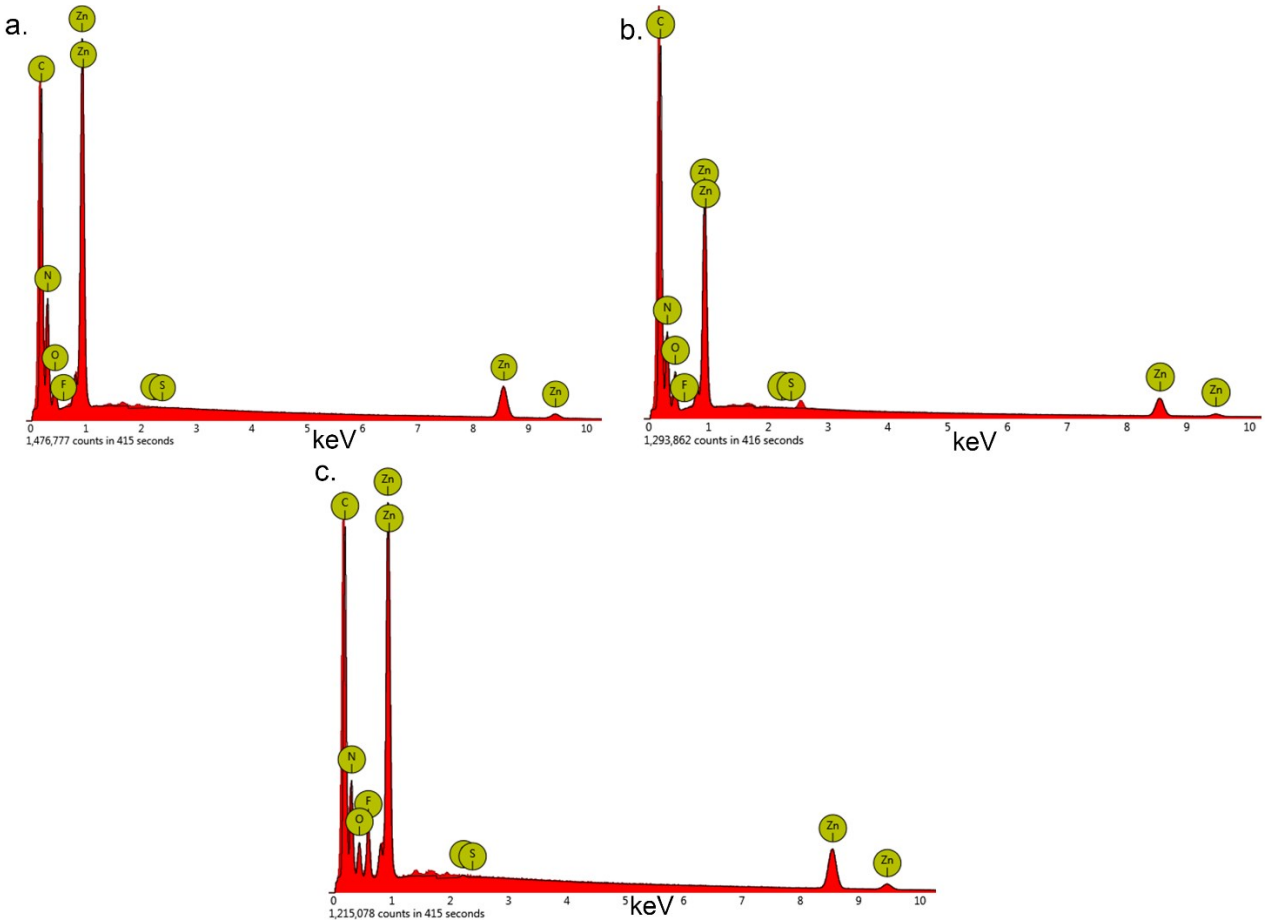

Figure S6. EDX spectra a. EZV, b. EZV-PEG and c. EZV-PFT sample. Only EZV-PFT sample displays a significant fluorine peak.

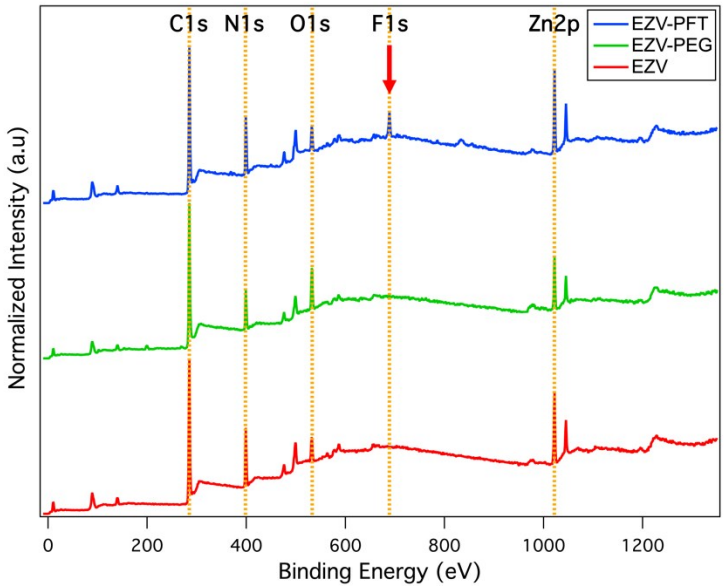

Figure S7. XPS survey scans of EZV, EZV-PEG, and EZV-PFT crystals. Only the EZV-PFT scan shows the appearance of a peak around 685eV, the location of an F1s bond.

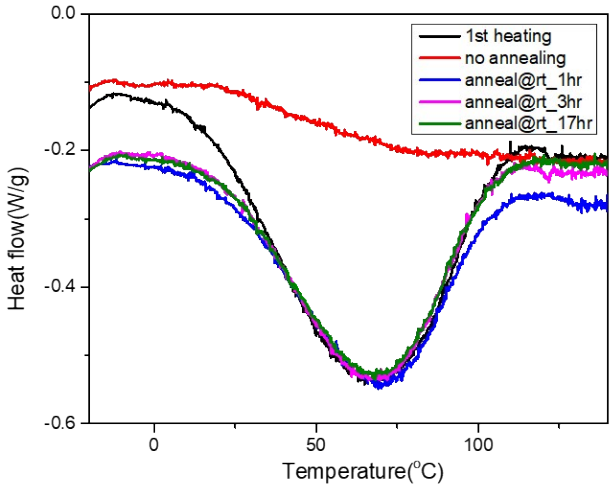

Figure S8. Repetitive heating of single EZ sample with varying anneal or cool-down periods. Phase-change depression phenomenon is preserved.

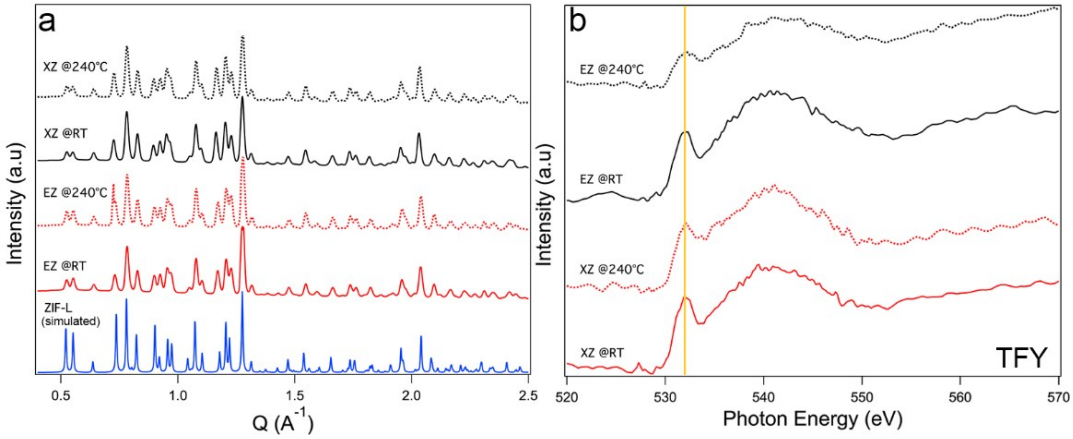

Figure S9. XRD (a) and XANES (b) data on XZ and EZ samples, collected at room temperature and 240 °C. Both XRD and XANES show little variance between spectra collected for the same sample at different temperatures, with shapes and positions of major peaks remaining constant.

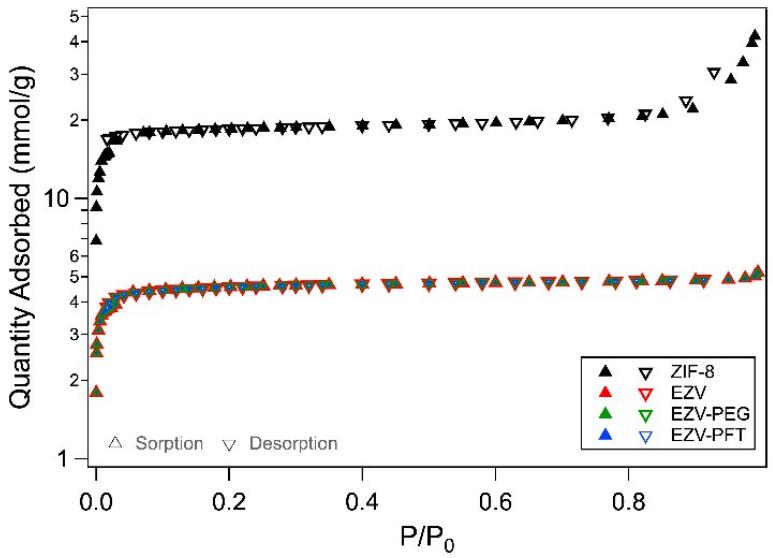

Figure S10. Nitrogen sorption and desorption isotherms for ZIF-8 (made in methanol) and EZV, EZV-PEG, and EZV-PFT (made in erythritol).

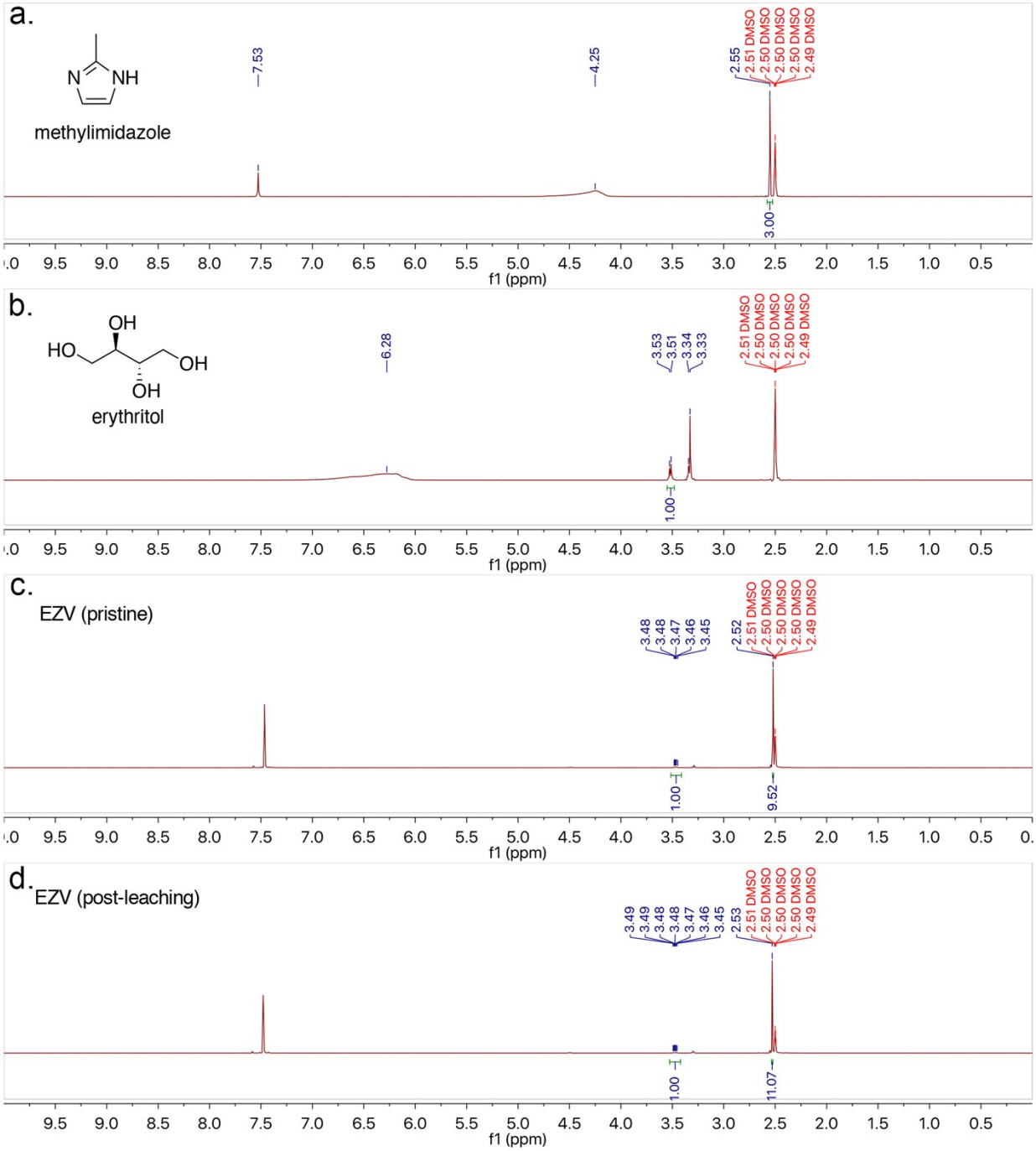

Figure S11. ^{1}H-NMR spectra of a. 2-methylimidazole, b. erythritol, c. pristine EZV, and d. EZV post-leaching test (DMSO-d_6 + two drops of D_2SO_4, 298K).

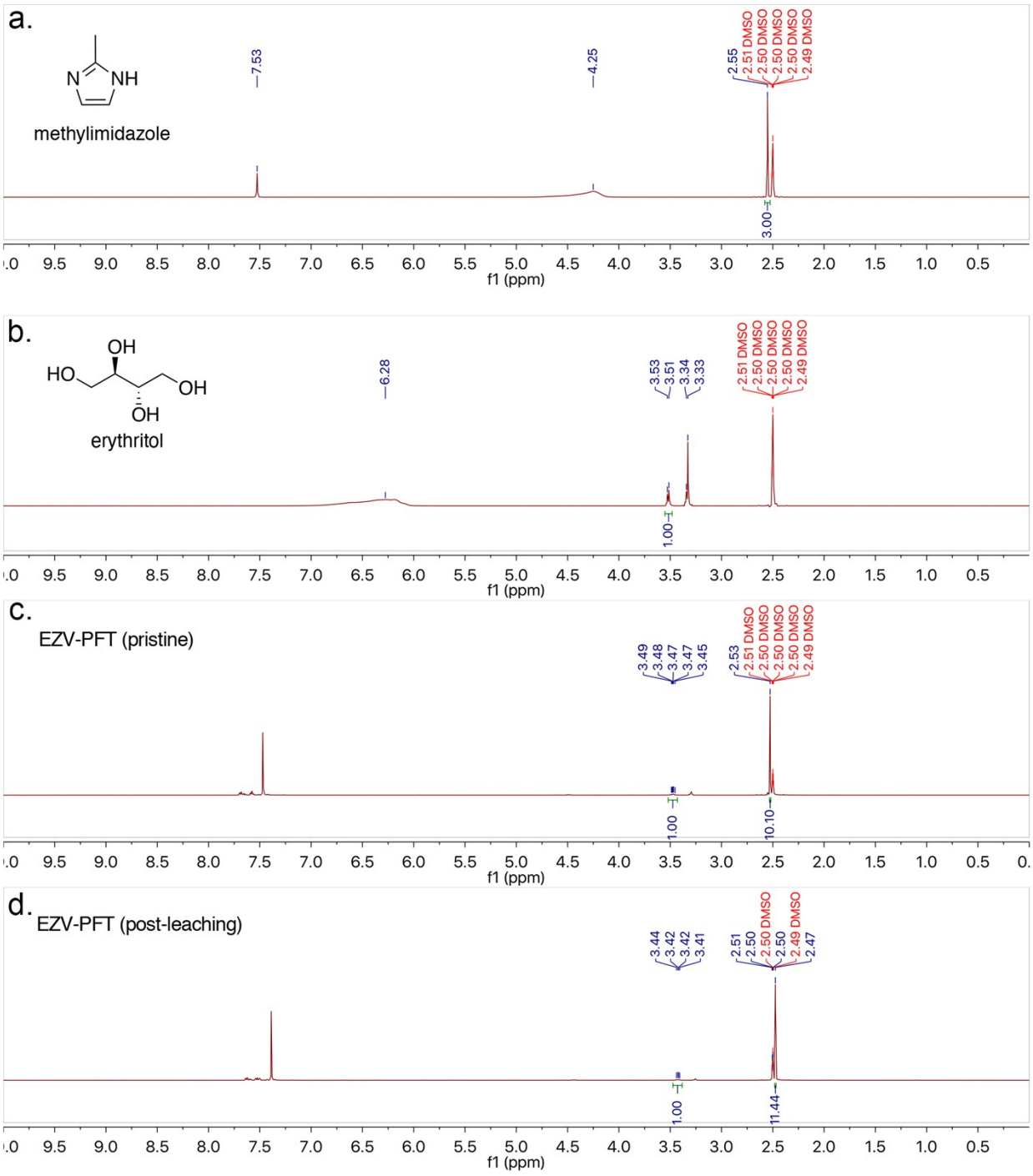

Figure S12. [1]H-NMR spectra of a. 2-methylimidazole, b. erythritol, c. pristine EZV-PFT, and d. EZV-PFT post-leaching test (DMSO-d6 + two drops of D_2SO_4, 298K).

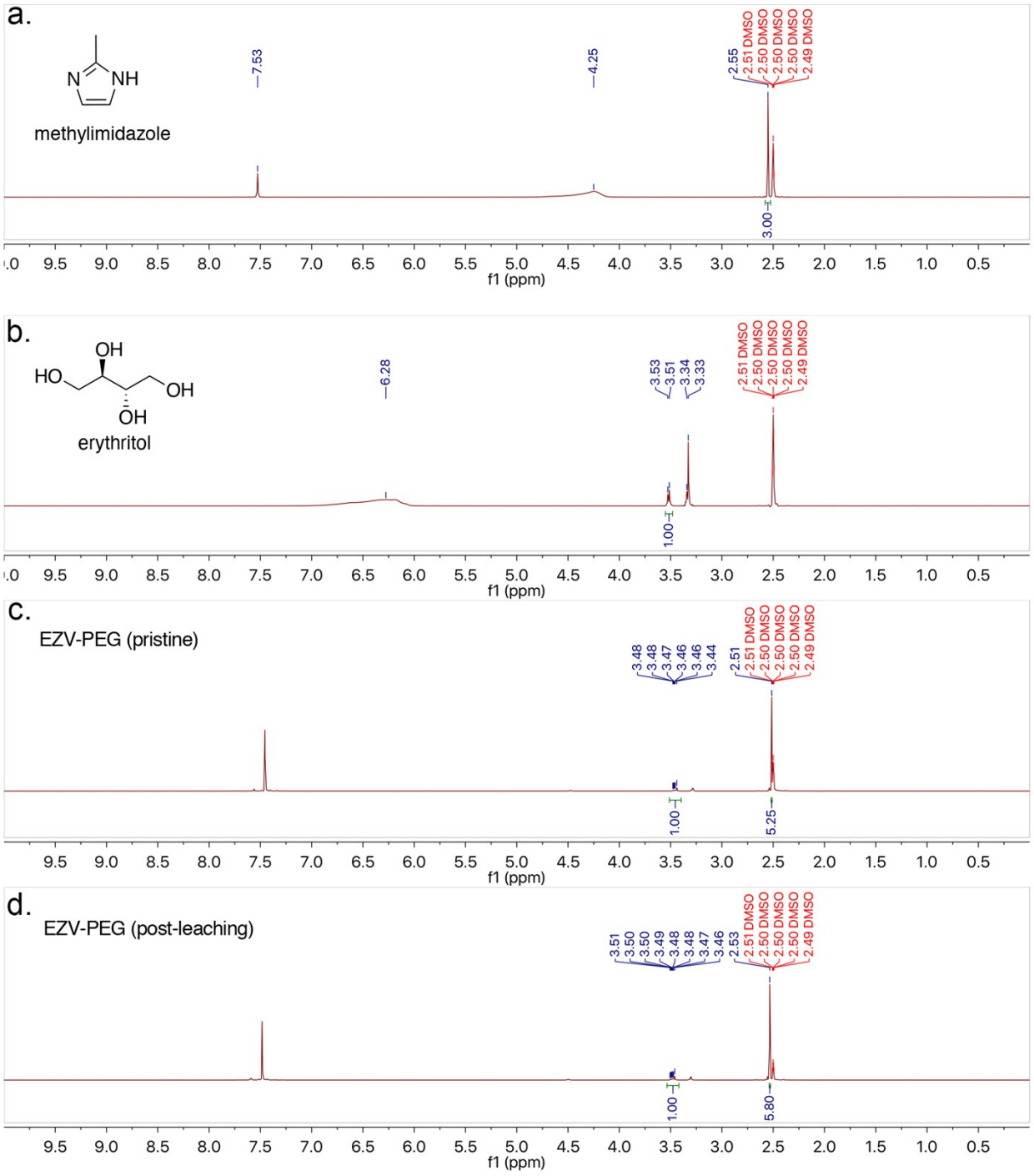

Figure S13. ^{1}H-NMR spectra of a. 2-methylimidazole, b. erythritol, c. pristine EZV-PEG, and d. EZV-PEG post-leaching test (DMSO-d6 + two drops of D_2SO_4, 298K).

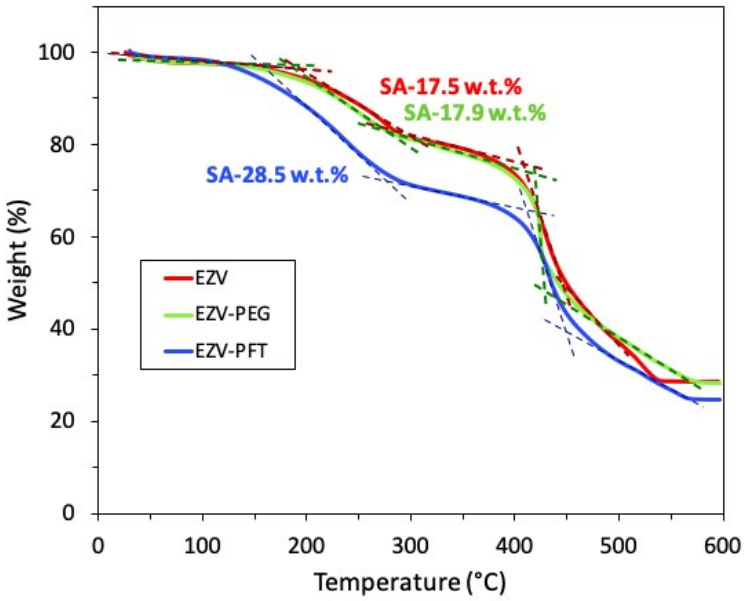

Figure S14. Sample weight loss as per TGA data of EZV, EZV-PEG and EZV-PFT. First major mass loss drop around erythritol melting point was used to estimate percentage erythritol loading capacity (in wt.% erythritol per g of given sample) of each sample, as indicated.

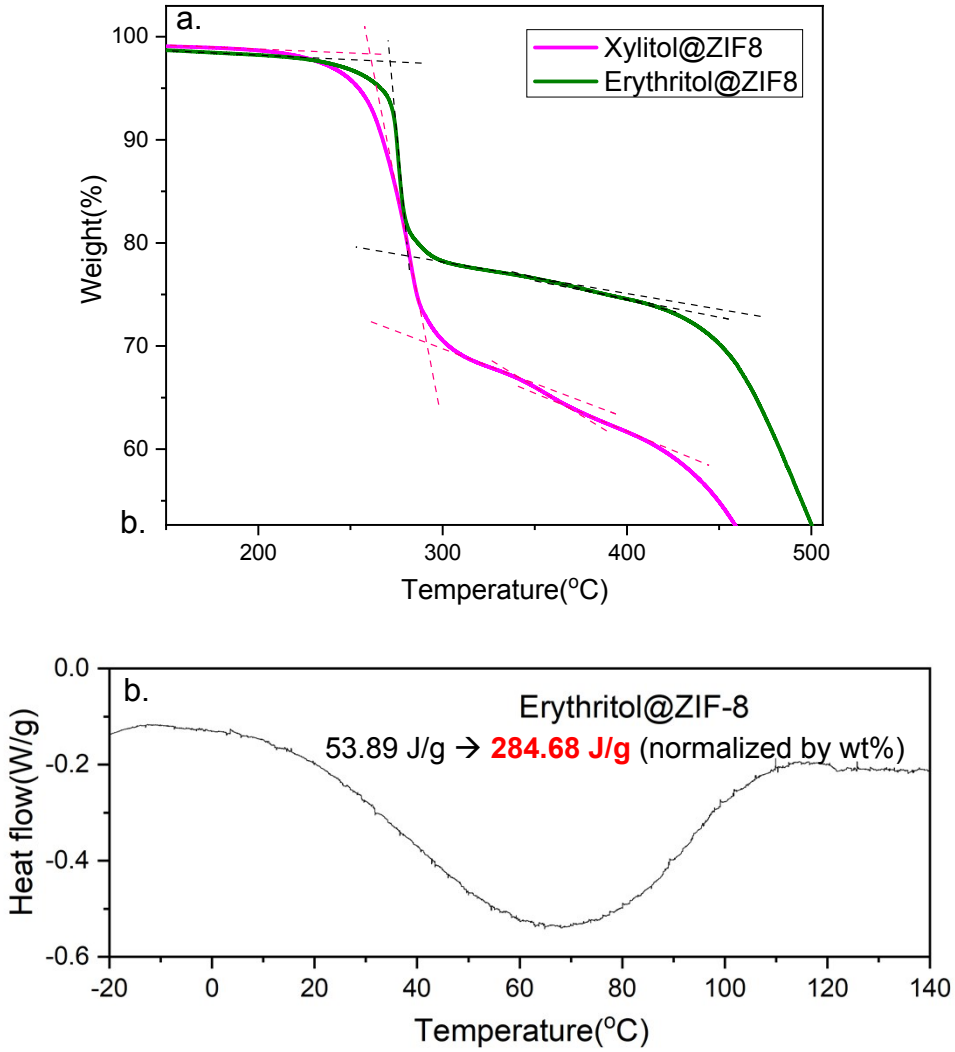

Figure S15. Illustration of latent heat normalization for the mass of SA contained in ZIF crystal. Panel a. illustrates the mass profile determined via TGA in response to the applied temperature profile. The mass of SA contained per sample was determined by looking at the % mass loss around the SA boiling points (~300 °C). The latent heat of the SA@ZIF assemblies were collected via DSC, as described in detail in the experimental section. The process is illustrated in panel b. for an erythritol@ZIF (EZ) sample. DSC peaks were integrated with the proprietary DSC software (TA Instruments Q1000) and then normalized by the mass percentage previously derived via TGA to normalize latent heat per g of contained SA.